

Coronal Mass Ejection of 26 February 2000: Complete Analysis of the Three-part CME Structure

D. Maričić¹, B. Vršnak², D. Roša¹, D. Hržina¹

¹Astronomical Observatory Zagreb, Opatička 22, HR-10000 Zagreb, Croatia

²Hvar Observatory, Faculty of Geodesy, Kačićeva 26, HR-10000 Zagreb, Croatia

E mail darije.maricic@zg.htnet.hr, drosa@zvjezdarnica.hr, dhrzina@zvjezdarnica.hr, bvrtnak@geodet.geof.hr

Accepted: 6 August 2012

Abstract. We analyze the kinematics and morphology of the limb coronal mass ejection (CME) of 26 February 2000, utilizing observations from Mauna Loa Solar Observatory (MLSO), the Solar and Heliospheric Observatory (SOHO) and the Geostationary Operational Environmental Satellite (GOES). Also, we analyze the relation between dynamics of the CME and the energy release in the associated flare.

An intricate structure (prominence, prominence-like absorbing feature, cavity and bright overlying arcade) is clearly recognizable in the low corona during the pre-eruption phase of slow rise. This provided measurements of kinematics of various features from the very beginning of the eruption up to the post-acceleration phase which was followed up to 32 solar radii. Such events are observed only occasionally, and are of great importance for the comprehension of the nature of forces driving CMEs. The acceleration maximum was attained at the radial distance of 2.4 solar radii from the solar center and ceased beyond 12 solar radii. The time profiles of the acceleration of various features of CME are showing "self-similar" expansion and implying a common driver. The acceleration phase was synchronized to a certain degree with the impulsive phase of the associated two-ribbon flare. Observations provide clear evidence that CME eruption caused a global restructuring of the magnetic field in the outer and inner corona. Furthermore, kinematics and morphological properties of this CME show possibility that in some events the prominence can evolve into a structure which looks like three-part structure CME, i.e. where the frontal rim is just a part of helically twisted prominence.

© 2012 BBSCS RN SWS. All rights reserved

Keywords: Sun: coronal mass ejection, MHD

Introduction

Coronal mass ejections (CMEs) are eruptions of large-scale coronal magnetic field structures. They are solar phenomena during which 10¹¹ – 10¹³ kg of coronal plasma is launched into interplanetary space at speeds ranging from several tens kms⁻¹, up to 2000 kms⁻¹. CMEs often expose a three-part structure: the prominence, the cavity and the leading edge [1], [2], [4], [7]. In this respect, observations in soft X-rays and the solar eclipse observation have revealed an analogue quiescent prominence / corona structure (the prominence is usually found in a coronal void nested in the helmet streamer), indicating that the basic CME morphology has its roots in the pre-eruption magnetic field configuration. Observations of CMEs show several evolutionary phases (see e.g., [5], [8], [10], [13]):

Slow rising motion (quasi-stationary evolution of the pre-eruptive structure through a series of equilibrium states).

The acceleration phase most often starts by an exponential-like development.

Post-acceleration phase, CMEs showing approximately constant velocity.

The association of CMEs and eruptive prominences provides important information regarding the process of initiation.

One of fundamental problems of these most spectacular events is that we still do not understand the physics of initiation, trigger mechanism, formation phase and the nature of forces driving the CMEs. What are the processes by which CMEs are

accelerated? Most probably, the mechanisms of eruption include catastrophic loss of equilibrium and some large-scale instability such as the MHD kink instability. It has been shown recently that process of eruption can be significantly affected by the process of reconnection below the rising flux-rope [3]. Our results are consistent with this hypothesis, since the acceleration of the CME was correlated with the energy release in the associated two-ribbon flare which is governed by the reconnection below the erupting flux rope [11].

In this paper, we present a detailed analysis of the kinematics of basic morphological features of the fast limb CME of 26 February 2000, from the pre-acceleration phase up to 30 solar radii. The CME is a relatively rare example where the entire erupting structure is recognizable already at low heights and these possibilities can be tested. A comparison of the height, speed, and acceleration time profiles of different components of CME provides an insight into the initiation process and the dynamics of CME until late phases of eruption. In addition, we analyze the relationship between the CME dynamics and the energy release in the associated flare.

The data set

The eruption 26 February 2000 was recorded by a number of ground-based and space-borne instruments. The FeXII 195Å images of the Extreme Ultraviolet Imaging Telescope (EIT) on board the Solar and Heliospheric Observatory (SOHO) are employed to measure the height of the EUV arcade overlying

the prominence. The HeI images recorded at the Mauna Loa Solar Observatory/High Altitude Observatory (MLSO/HAO) are used to follow the kinematics of the upper edge of the prominence. Data from the Soft X-Ray Telescope (SXT) aboard the Yohkoh satellite are utilized to inspect the morphology of the event in the pre-eruption phase. The soft X-ray (SXR) flux measurements in the 1-8 Å and 0.5-4 Å channels of the Geostationary Operational Environmental Satellite (GOES) are used

to get information on the energy release in the associated flare.

The eruptive prominence is traced through the inner corona utilizing the H α and white-light images gained by the MK-IV K-coronameter of the Mauna Loa Solar Observatory (MLSO). Also, white-light data acquired by the Large Angle and Spectrometric

Coronagraphs (LASCO) on board SOHO, are used to follow the three-part structure of the CME from the inner corona to the interplanetary space.

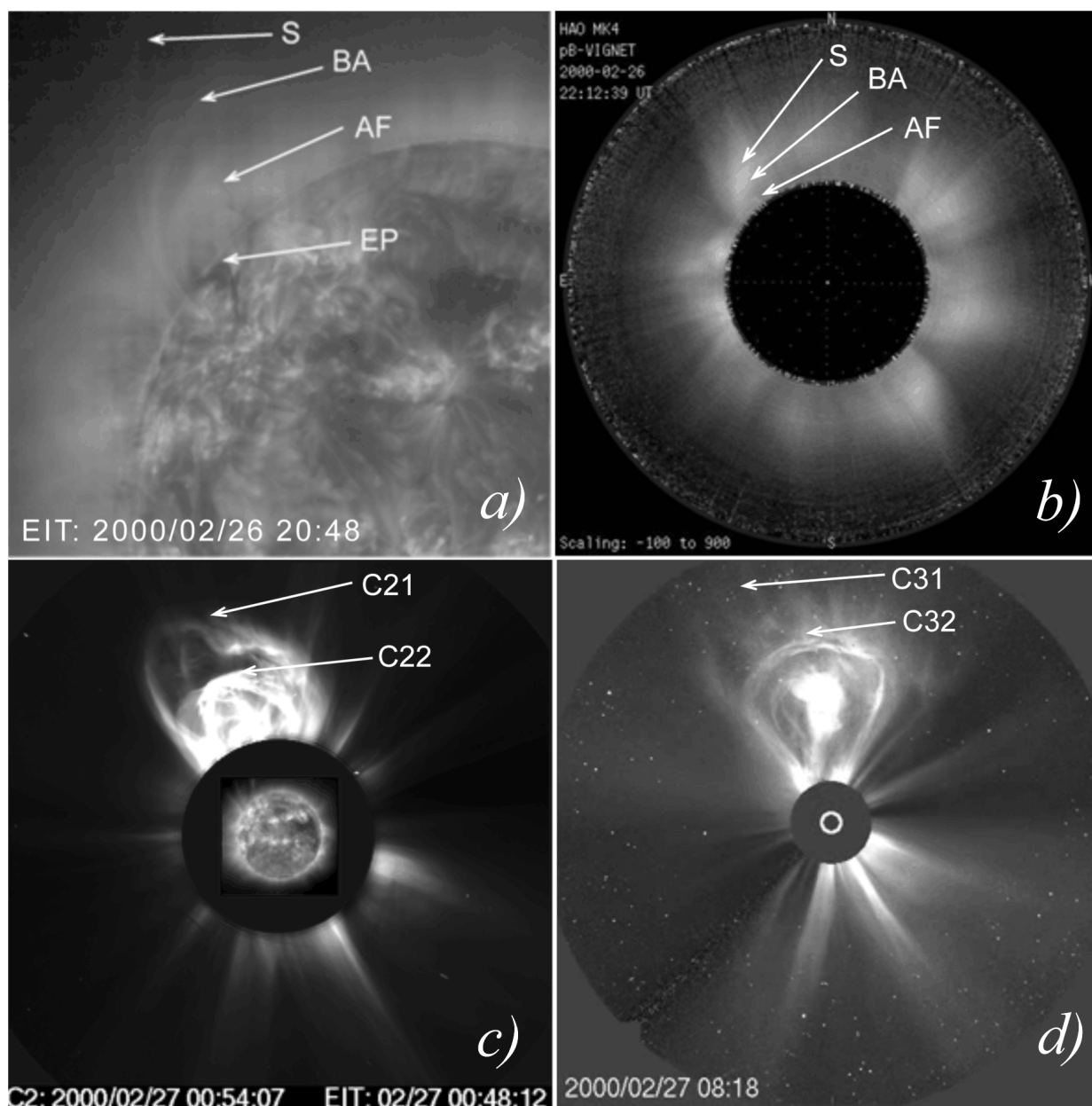


Fig. 1. a) The CME formation observed by EIT (FeXII 195A) image: EP - the eruptive prominence, AF - absorbing prominence-like feature, BA - bright arcade and S - a part of the streamer. Top is north and left is east, the same for all figures in this paper. b) The CME formation observed by MKIV Koronameter from Mauna Loa Solar Observatory. The labeling is the same as in EIT (FeXII 195A) image. c) The evolution of the CME in white light LASCO-C2 coronagraph image. The image shows regular CME with three-part structure. d) The evolution of the CME in white light LASCO-C3 coronagraph image

The morphology of the 26 February 2000 event

Pre-eruption evolution

The prominence and bright overlying coronal loops appeared in EIT images above north-east solar limb on 24 February 2000. The filament was embedded in a large scale magnetic arcade of EUV loops, extending up in the plane of sky to the projection heliocentric distance of 1.23 solar radii below a helmet streamer extending outwards at the position angle $PA \approx 30^\circ$. In this CME the streamer is believed to be a simple open arcade structure before the eruption, which is no longer visible after the CME take-off. The quiescent filament was

extending in the north-east direction between the active regions NOAA 8889 and NOAA 8888, located at 25N56E and 32N49E on 2000 February 25, respectively. The active region NOAA 8889 was containing a sunspot group, which was classified as spot class Es: bipolar with symmetric penumbra; while the active region NOAA 8888 was containing only a minor spot. One of the filament foot-points was located at 34N55E and another at 37N, at the very E-limb, corresponding to the radial coordinates of 0.9 solar radii and 1 solar radii, respectively. Filament foot-points did not coincide with the foot-points of the pre-event EUV loops which were overlying it. get the real value of height h^* or heliocentric distance r^* .

Since this is well below the errors of measurements in the following we take h approx h^* and r approx r^* . All EIT features whose kinematics was followed are marked in Fig.1a, which is a overview of arcade morphology as recorded in FeXII 195A line by EIT. Thus, there is a clear observational evidence from EIT images, that in the pre-eruption phase, the common prominence/corona structure existed: the prominence (EP), the absorbing feature (AF), the overlying bright arcade (BA), and the streamer (S). We note that structure was highly active in preceding days: several flares, small CMEs and dynamical interactions with neighbouring magnetic field, were observed. A formation of relatively intense EUV loops can be attributed to this activity. The EUV loops were gradually transforming through 2000 February 24-26. Initially intertwined loops were becoming more and more parallel. This process was accompanied by formation of irregular absorbing prominence-like features (AF) above the filament, which on the other hand, showed only a minor activity in this period. This features first become visible at 09:00UT on February 26 and are indicated in Fig.1a (20:48 UT frame).

The structural change of the EUV loops was accompanied by "swelling" of the loops resulting in a slow rise of the loops summit.

The transformation of the EUV loops into a homogeneous bright arc (BA) was completed several hours before the eruption. Its summit was at 1.23 solar radii from the solar center. Below the bright arcade a region of decreased intensity, presumably the cavity, was formed. Within the cavity, a prominent absorbing

feature AF was located at the 1.16 solar radii from the disc center. Finally, a rising core - the prominence (EP) is observed as the lowest recognizable coronal feature. The top of the prominence was at the projected radial distance of 0.98 solar radii from the disc center. We estimated the average rising velocity between 08:00-23:00UT on February 26 of the bright arc and the absorbing feature AF as 1.6 km/s and 0.6 km/s, respectively.

The prominence showed only a minor motion in this period, with no global trend (upward). The structure was expanding in a self-similar manner, not changing the overall shape or the internal structure significantly.

Acceleration phase

The onset of the acceleration phase of the prominence eruption can be located into the period between the two EIT images taken at 23:12 and 23:24 UT. It is worth noting that the prominence eruption started at the position angle $PA \approx 52^\circ$ whereas later on, in the C2 and C3 field of view the CME was propagating along the position angle $PA \approx 10^\circ$, i.e., in a predominantly northward direction. Thus, the motion was not purely radial during the acceleration phase of eruption. The bright arc (BA) can be followed only in EIT images, thus we were not able to monitor it in the acceleration phase since its summit left the EIT field of view. The prominence finally disappeared from the EIT field of view at 00:24 UT on February 27. At larger heights, the CME was tracked by the white light LASCO C2 and C3 coronagraphs. The measured CME features in LASCO C2 images are denoted as C21 and C22 (Fig.1c, 00:54:07 UT frame). The CME entered the LASCO C2 field of view at 00:06 UT on February 27, rising below a pre-existing coronal streamer. Between 00:06 and 01:54 UT on February 27 the irregular dim feature (C21) are seen above the bright core (C22) which shows a three-part structure. The CME feature marked by C22 could be tracked in LASCO-C2 until 02:30 UT when it left the C2 field of view. LASCO C2 images clearly show that what is seen as the bright frontal loop in low resolution (top is denoted as C22 in Fig.1c), is not a simple structure, but rather exposes a prominence-like helical patterns. Furthermore, there is thin filamentary feature (C21) which connects the bright loop with the inner structure (C22). Thus, the structure of the outer envelope cannot be interpreted as an overlying arcade. The CME entered in the C3 field of view at 00:42 UT on February 27. The CME features measured in the LASCO C3 images are denoted as C31 and C32 (Fig.1d, 08:18 UT frame). In the LASCO C3 images the CME is observed to develop similarly as in C2 field of view, showing the three-part structure that consisted of an outer expanding bright circular rim (C32) surrounding a relatively dark cavity and the bright core. Yet, ahead of the bright frontal rim, irregular dim features (C31) are observed. Intensity of the irregular features was decreasing with the

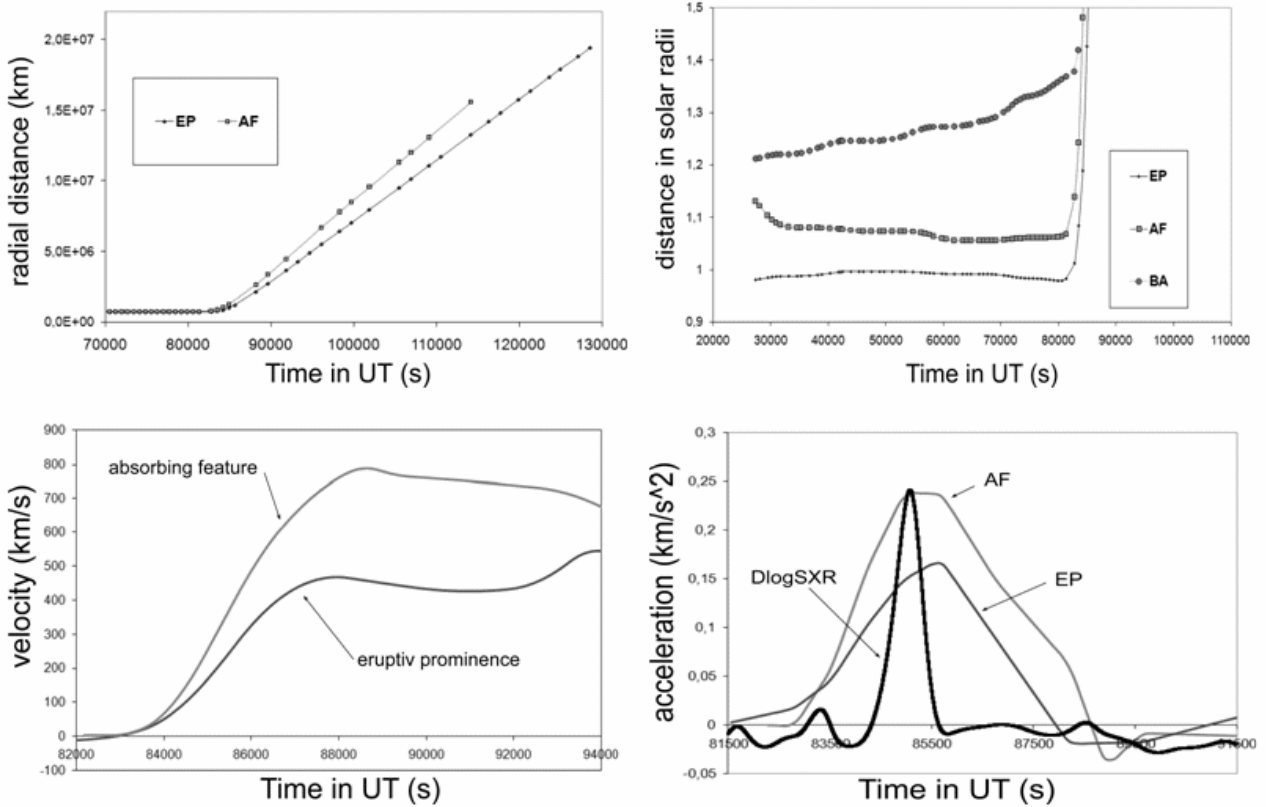


Fig. 2. a) The smoothed height-time plot for absorbing feature and the top of the prominence as measured from the LASCO C2/C3, MKIV and EIT images. b) Kinematics of the EP - the eruptive prominence, AF - absorbing prominence-like feature and BA - bright arcade, during the pre-acceleration phase. c) The velocity-time plot for absorbing feature and the top of the prominence. d) The acceleration-time plot for absorbing feature and the top of the prominence compared with the derivative of the associated flare SXR flux.

distance, and at distance of 22 solar radii are not recognizable any more. Around 12:42 UT the last measured feature (C32) left the C3 field of view. In the LASCO C3 domain, between 5 to 32 solar radii, CME was expanding out along the position angle $PA=10^\circ$ and all measured features had a velocity between 400 - 800 km/s.

Kinematics of the CME

The analysis of the kinematics is focused on the distance-time measurements of the top of the bright arcade, the top of the absorbing features and the top of the eruptive prominence. For each morphological feature measured in EIT, MKIV, C2, and C3 the $h(t)$ curves are shown in Fig. 2. The identification of the respective features was accomplished by comparing and matching their kinematical curves $h(t)$, combined with the inspection of their structural characteristic. From examination of EIT, MKIV and LASCO images and from the performed fits it is found that: (i) the top of the prominence (EP) seen in EIT corresponds to the C22 feature in LASCO-C2 images and C32 feature in LASCO-C3 images, i.e., with the top of the feature which looks like the bright frontal rim of CME; (ii) the absorbing feature (AF) seen in EIT Fe XII 195A line corresponds to the feature C21 in LASCO-C2 images and C31 feature in LASCO-C3 images; (iii) for the bright arc (BA) seen in EIT images

we did not find a counterpart in LASCO-C2 and C3 images.

After the corresponding features in EIT, MKIV and LASCO C2/C3 images were properly associated, the data were joined for a given feature and smoothed. The smooth function uses a symmetric k nearest neighbor linear least-squares fitting procedure (in which k is adaptively chosen) to make a series of line segments through our data [5]. Then we have determined speed by using two successive smoothed data points:

$$v(t_{vi}) = (r(t_{i+1}) - r(t_i)) / (t_{i+1} - t_i) \quad (1)$$

where $r(t_i)$ is the height at time t_i and $t_{vi} = (t_{i+1} + t_i) / 2$. The obtained speed-time dependence is then again smoothed. In the following step, we have determined the acceleration applying:

$$a(t_{ai}) = (v(t_{vi+1}) - v(t_{vi})) / (t_{vi+1} - t_{vi}) \quad (2)$$

where $v(t_{vi})$ is the height at time t_{vi} and $t_{ai} = (t_{vi+1} + t_{vi}) / 2$.

Comparison of the overall height-time plots for the absorbing feature and the prominence top is shown in Fig. 2a, featuring the basic representation of the CME motion. The height-time plot, which is covering the observations only up to 1.5 solar radii is shown. This height-time plot indicates approximately self-similar expansion of all features in the low corona. The rise of

the bright arcades in region below 1.5 solar radii is continuous, while prominence and absorbing feature (AF) show motion which can be attributed solely to a projection effect caused by solar rotation.

The velocity-versus-time plot is similar for the prominence and absorbing feature (Fig. 2c). This suggests that all parts of CME are driven by a common process. The absorbing feature and the prominence attained at the height of 4 solar radii a relatively high velocity of about 780 km/s and 470 km/s, respectively. This is probably faster than the ambient solar wind, which [6] found to be roughly 100-200 km/s in C2 field of view and roughly 200-300 km/s in the C3 field of view. From Figure 2c, it is seen that the prominence at any instant of time is slower than the absorbing features. For this particular CME the acceleration takes place below height of 4 solar radii. Kinematical curves indicate that the absorbing feature is gradually slowing down (decelerating) beyond 9 solar radii. This is not surprising, since the CME is plowing through a much slower solar wind. The acceleration becomes negative and speed slows down for AF from 780 to \approx 600 km/s.

From Figure 2b, one notices that all CME measured features started to accelerate approximately at the same time into the period between the two EIT images taken at 23:00 and 23:12 UT February 26. However, the maximum acceleration of EP ($a=165 \text{ m/s}^2$) was lower than the maximum acceleration of the absorbing feature AF ($a=235 \text{ m/s}^2$). Figure 2d shows the acceleration-versus-time plot for this event. Fig. 2d, shows that acceleration reaches the maximum values approximately at the same time (between 23:24 - 23:36 UT) at a height between 2.3 and 2.5 solar radii for all measured features. It can be noticed that the AF and EP acceleration rises from almost zero to 165 m/s^2 and 235 m/s^2 , respectively.

In Figure 2d we also show the acceleration-time plot for all absorbing feature and top of the prominence simultaneous with the derivative of the associated flare SXR flux. This CME belong to category of event in which the acceleration phase and the SXR burst growth were synchronized to a certain degree. CME shows simultaneity of the acceleration maximum and the peak of the the GOES 0.5-4Å SXR flux derivative, but the acceleration phase lasted approximately five times longer than the SXR flux growth.

Discussion and Conclusion

We have presented the morphology, initiation, and kinematics of a slowly evolving CME on 2000 February 26. The CME is associated with a dramatic prominence eruption. This CME was chosen for our analysis partly because it has a regular three-part structure in LASCO observation, while in EIT it has a much more complicated structure. The presented multi-wavelength analysis of the eruption shows that this event could be considered as a typical example

of a gradual CME [13]. We summarize the results as follows:

- The structure was expanding in a self-similar manner, not changing the overall shape or the internal structure significantly.
- In the pre-eruption phase, the common prominence/corona structure existed: the prominence (EP), the absorbing feature (AF), the overlying arcade (BA), and the streamer (S).
- The absorbing feature (AF), and the prominence attained at the height of 4 solar radii a relatively high velocity of about 780 km/s and 470 km/s, respectively.
- The maximum acceleration of the prominence ($a=165 \text{ m/s}^2$) was lower than the maximum acceleration of the absorbing feature ($a=235 \text{ m/s}^2$).
- The acceleration phase is synchronized to a certain degree with the growth of the associated SXR flare.
- Kinematics and morphological properties of this CME show possibility that in some events the prominence can evolve into a structure which looks like three-part structure CME, i.e., where the frontal rim is just a part of helically twisted prominence.

We would like to thank the GOES, MLSO and SOHO teams for developing and operating the instruments and we are grateful for their open data policy.

References

- Chen, J.: 1989, *Astrophys. J.* 338, 453.
 Fisher, R. and Poland, A.I.: 1981, *Astrophys. J.* 246, 1004.
 Lin, J., Raymond, J.C., and van Ballegooijen, A.A.: 2004, *Astrophys. J.* 602, 422.
 Low, B.C., Munro, R.H., and Fisher, R.R.: 1982, *Astrophys. J.* 254, 335.
 Maričić, D., Vršnak B., Stanger, A., and Veronig, A.: 2004, *Solar Phys.* 225, 337.
 Sheeley, , N.R.Jr., Wang, Y.-M., Hawley, S.H. et al.: 1997, *Astrophys. J.*, 484, 472.
 Srivastava, N., Schwenn, R., Inhester, B., Martin, S.F., and Hanaoka, Z.: 2000, *Astrophys. J.* 534, 468.
 Vršnak B.: 2001, *J. Geophys. Res.* 106, 25249.
 Vršnak B.: 2001, *Solar Phys.* 202, 173.
 Vršnak B., Maričić, D., Stanger, A., and Veronig, A.: 2004, *Solar Phys.* 225, 355.
 Wood, B.E., Karovska, M., Chen, J., Brueckner, G.E., Cook, J.W., and Howard, R.A.: 1999, *Astrophys. J.* 512, 484.
 Zhang, J., Dere, K.P., Howard, R.A., Kundu, M.R., and White S.M.: 2001, *Astrophys. J.* 559, 452.
 Zhang, J., Dere, K.P., Howard, R.A., and Vourlidas, A.: 2004, *Astrophys. J.* 604, 420.